Propagation Behavior of Root Crack in Restraint Cracking Test on the Basis of AE Source Location Technique†

– Application of Acostic Emission Technique for Weld Cracking (II) –

Fukuhisa MATSUDA*, Hiroji NAKAGAWA** and Yoshinori MORIMOTO***

Abstract

AE source location technique is applied to restraint cracking test with single bevel groove for 80kg/mm² class high strength steel. The AE data are analyzed in relation to time and location of cracking in order to reveal the propagation behavior of the root crack. Consequently relationship between the crack ratio and the characteristics of AE parameters, changes in AE source location and other AE parameters vs. time, and dependence of average cracked area per AE event on the propagation mode of root crack, and so on are presented. Moreover, propagation behavior of the root crack is discussed from a synthetic judgement on the AE parameters obtained.

1. Introduction

Root crack is one of the most serious problems in welding of high strength steel. Therefore many efforts have been made through many years in order to reveal its cause and to prevent its occurrence from metallurgical and mechanical viewpoints. Consequently many fruitful results have been obtained, but there have been yet remaining many unsolved problems. One of the unsolved problems is propagation behavior of the root crack.

Recently it has been reported[1-7] that acoustic emission (AE) technique is useful to monitor cold crack in welded zone such as the root crack in real time, since the cold crack is a hydrogen-induced delayed crack and thus high amplitude AE are given off during the crack propagation[8, 9]. In these reports, however, AE source location technique was not used and thus the AE data were analyzed in relation to only time without information about cracking position. On the other hand, the authours showed in the previous paper[10] that application of AE source location technique to weld cold crack is nearly satisfactory even in a small sized specimen.

Therefore in this report AE source location technique is applied to restraint cracking test of 80kg/mm² class high strength steel, and the AE data are analyzed in relation to time and location of cracking in order to reveal the propagation behavior of the root crack.

2. Materials Used and Experimental Procedures

A weldable heat-treated high strength steel HT80 whose ultimate strength was 80kg/mm² was used for the restraint cracking test. The chemical composition is shown in **Table 1**. The configuration of test specimen is shown in **Fig. 1**, in which a single bevel groove was machined in order that the root crack mainly passes the heat-affected zone. The restraint welding in both sides of the groove was done with electron beam welding by each one pass from top and back surfaces. Restraint intensity in a restraint cracking test specimen is usually varied by cutting parallel slits from the longer edges of the specimen[11]. It is feared in this study, however, that the slits change the acoustic characteristics of the specimen to a considerable degree. Therefore the restraint intensity in this study was varied by changing the groove length L in Fig. 1. The selected L values were 120, 150 and 180mm. The restraint intensities with L of 120, 150 and 180mm are about 1800, 1100 and 600 kg/mm.mm respectively at the middle of each groove length according to the formula in case of uniformly distributed loads derived by Ueda et al[12], though the dimensions of the specimen in Fig. 1 lie in somewhat outer zone of the applicable range.

Shielded metal-arc welding was done using AWS E11016 low hydrogen type electrode. The chemical composition of the deposited metal is shown in Table 1. Baking condition of the electrode and preheating temperature of the test specimen were varied in order to

† Received on Oct. 20th, 1978
* Professor
** Research Instructor
*** Graduate Student of Osaka Univ.

Table 1 Chemical compositions of base metal and deposited metal

Material	Composition (wt.%)										
	C	Si	Mn	P	S	Cu	Ni	Cr	Mo	V	B
Base metal	0.12	0.26	0.84	0.008	0.006	0.22	0.91	0.48	0.42	0.04	0.0013
Deposited metal	0.06	0.63	1.36	0.010	0.005	–	1.73	0.24	0.44	–	–

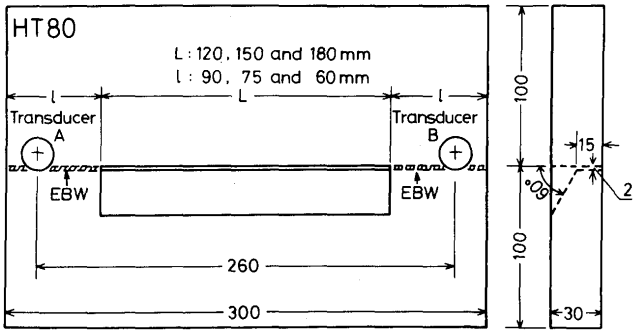

Fig. 1 Specimen configuration of restraint cracking test with single bevel groove

obtain various crack sizes. The starting part and the crater of the weld bead were turned away from the root gap to avoid weld defects. The welding condition was 150mm/min of welding speed, 170A of welding current and 25V of arc voltage. Immediately after the welding slags on the bead surface were completely removed.

Then, two AE transducers were set on the test specimen as shown in Fig. 1 and AE measurement was started from 2 min after the completion of welding. The temperature of welded zone at this moment was about 70°C without preheating condition. The AE monitoring system has dual channels, which is just the same as that used in the previous paper[10]. Briefly describing, the transducers were differential type having flat response and sensitivity of –84dB referred to 1V/μbar, the bandpass filters were selected from 100 to 350kHz, and the total gain was set to 70dB. The procedure to calibrate the AE source location was the same as that used in the previous paper[10].

Major AE parameters measured were AE cumulative count which was defined as sum of ringdown counts over 1 volt threshold, AE comulative event count which was defined as sum of number of AE bursts over 1 volt threshold, and AE source location. Besides, the maximum ringdown counts per event and S value were also measured. The S value is the slope of a ringdown counts distribution where the plots are logarithm of the sum of events which have ringdown counts exceeding a given value as a function of this value. Small S value means that there are comparatively many events having large ringdown counts in the ringdown counts distribution. The ringdown counts distribution has the similar meaning to that in the AE amplitude distribution[13].

AE measurement was stopped after the testing of 48hr and the specimen was immediately taken into an electric furnace of about 350°C in order to oxidize the crack surface. Subsequently the specimen was fractured by a bending test machine at room temperature. As regards fully cracked specimen, however, the oxidizing was omitted. Then various crack ratios were measured on the fractured surface.

The crack ratio on fractured surface Ca was defined as follows:

$$Ca = Ac/As \times 100\ (\%) \quad \ldots\ldots (1)$$

where, Ac; cracked area
As; sum of cracked and fractured area.

The cross sectional crack ratio Cs was defined as follows:

$$Cs = \frac{1}{N} \sum^{N} Hc/Hb \times 100\ (\%) \quad \ldots\ (2)$$

where, N; measured number (selected to five in equal distance for the weld bead)
Hc; height of root crack in cross section
Hb; height of weld bead in cross section.

The surface crack ratio Cf was defined as follows:

$$Cf = \Sigma Lf/L \times 100\ (\%) \quad \ldots\ldots (3)$$

where, ΣLf; total length of cracks on the surface of weld bead
L; length of weld bead.

The root crack ratio Cr was defined as follows:

$$Cr = \Sigma Lr/L \times 100\ (\%) \quad \ldots\ldots (4)$$

where, ΣLr; total length of cracks at the root.

3. Experimental Results and Discussions

3.1 Results of Restraint Cracking Test

Table 2 shows summary of the results of the restraint cracking test and the AE data. Increasing the restraint intensity or lowering the baking condition of electrode and the preheating temperature of specimen increased the crack ratios.

Root crack of fully cracked specimen occurred at the root, propagated nearly linearly in the heat-affected zone and turned into the weld metal as a shear lip mode, an example of which is shown in **Fig. 2 (a)**. A part of the root crack of fully cracked specimen with the highest restraint intensity, however, propagated nearly linearly from the heat-affected zone to the weld metal before turning as a shear lip, an example of which is shown in **Fig. 2 (b)**.

Table 2 Summary of the results of restraint cracking test and AE measurements

Specimen number	Restraint intensity (kg/mm·mm)	Baking condition of electrode (°C x hr)	Preheating temperature (°C)	Cracked area (mm^2)	Crack ratio* (%)				AE data			
					Ca	Cs	Cf	Cr	Cumulative count**	Cumulative event count	S value	Max. ringdown counts/event
1	600	380 x 3	room temp.	2	0.2	1	0	1	3400	28	1.45	1600
2	600	350 x 2.5	100	3	0.3	0	0	4	12500	35	0.92	3100
3	600	370 x 1.6	90	4	0.4	0	0	7	37700	122	1.05	3700
4	600	390 x 3	room temp.	11	1	0	0	15	13000	79	1.65	2100
5	600	230 x 1	room temp.	28	3	1	0	35	38200	94	0.85	4400
6	600	240 x 0.5	room temp.	414	42	46	0	98	21700	94	–	3000
7	600	240 x 1	room temp.	773	80	75	58	98	313700	237	0.53	8600
8	600	as received	room temp.	971	100	100	100	100	823800	478	0.35	>10000
9	600	as received	room temp.	988	100	100	100	100	609700	386	0.45	>10000
10	1100	360 x 1.3	room temp.	4	0.4	0	0	10	14500	67	1.20	2700
11	1100	360 x 1.5	50	4	0.5	0	0	12	11500	56	1.55	1900
12	1100	360 x 1.3	room temp.	187	23	26	0	75	2400	31	>3	600
13	1100	340 x 1.5	room temp.	326	42	34	0	95	12500	57	1.45	2000
14	1100	160 x 1.1	room temp.	838	100	100	100	100	294300	229	0.42	>10000
15	1800	370 x 1.3	75	4	0.6	1	0	14	8400	34	1.28	2000
16	1800	360 x 1.8	room temp.	200	31	36	0	100	14400	37	0.62	5000
17	1800	360 x 1.3	room temp.	328	51	47	0	100	25100	61	0.60	5900
18	1800	330 x 1.7	room temp.	354	63	56	8	100	32800	67	0.95	3500
19	1800	240 x 1	room temp.	655	100	100	100	100	454500	245	0.42	>10000

* Ca is crack ratio on fractured surface, Cs is cross sectional crack ratio, Cf is surface crack ratio and Cr is root crack ratio.

** AE cumulative count is the mean value of two channels.

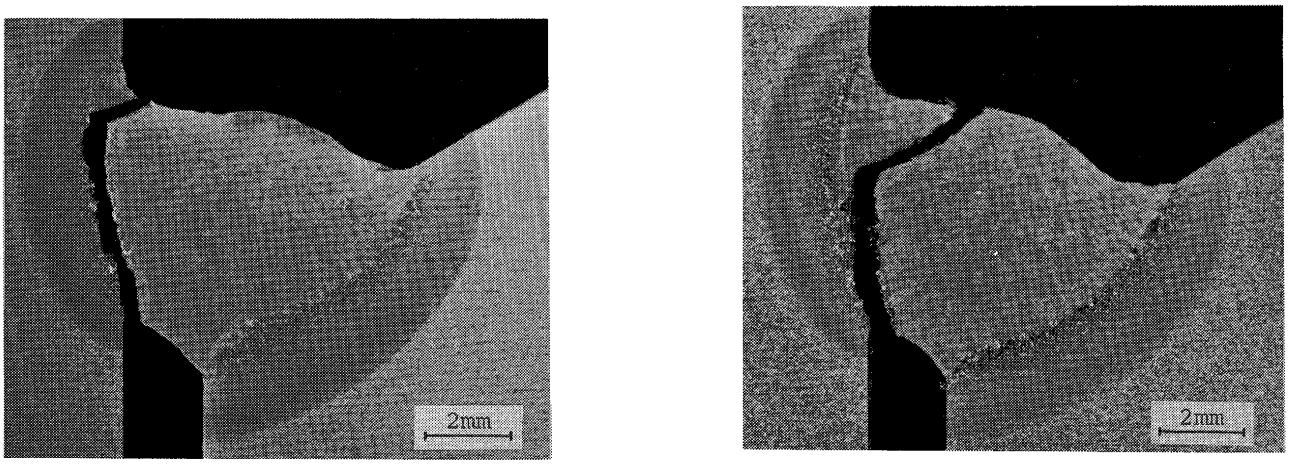

(a) with the lowest restraint intensity

(b) with the highest restraint intensity

Fig. 2 Macrostructure of transverse cross section of welded zone in fully cracked specimen

3.2 AE Source Location during Cracking Test

Characteristics of AE source location and AE other parameters depended on the crack ratios and were classified into three groups, that is Groups I, II, and III. The characteristics of AE in a specimen with a large crack ratio Ca in which surface crack ratio Cf was also large

belonged to Group I. That in a specimen with a medium crack ratio Ca in which there was no or a little surface crack but was nearly full crack at the root belonged to Group II. That in a specimen with a small crack ratio Ca in which there were generally only some tiny cracks at the root belonged to Group III. The relationship between the various crack ratios and these groups is shown in **Fig. 3**.

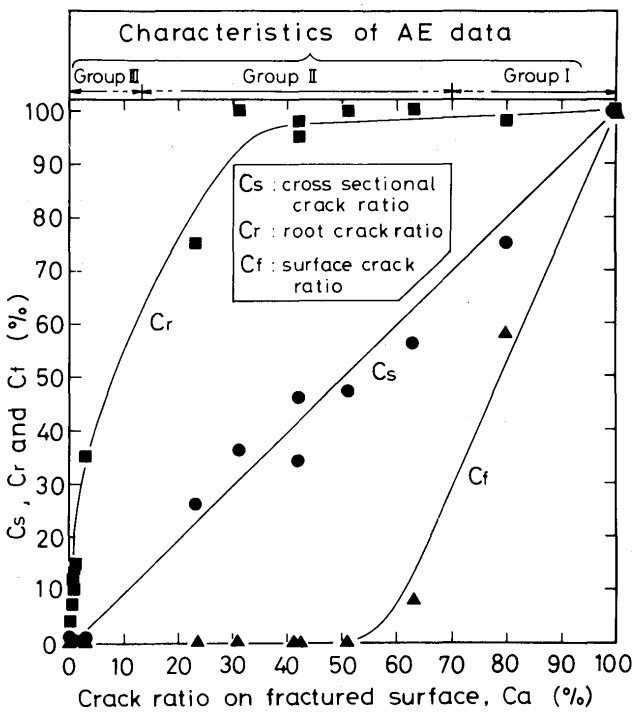

Fig. 3 Relationship between various crack ratios and characteristics of AE data

In the following, the AE data are described according to this classification.

3.2.1 AE Source Location in Group I

As an example, **Fig. 4** shows the changes in AE cumulative count and AE cumulative event count vs. time in specimen No. 8 and **Fig. 5** shows the change in AE source location in the same specimen during the time intervals shown in Fig. 5. Relative location in the abscissa in Fig. 5 is defined to be 0% at the left transducer and 100% at the right one in Fig. 1, and the increase in the relative location agrees with the welding direction. Considering the error in AE source location in the AE monitoring system used[10], the AE emitted in the weld metal must be lie between about 10 to 90% of relative location, the range of which is indicated by arrows in Fig. 5.

In Fig. 4 AE were emitted immediately after the start

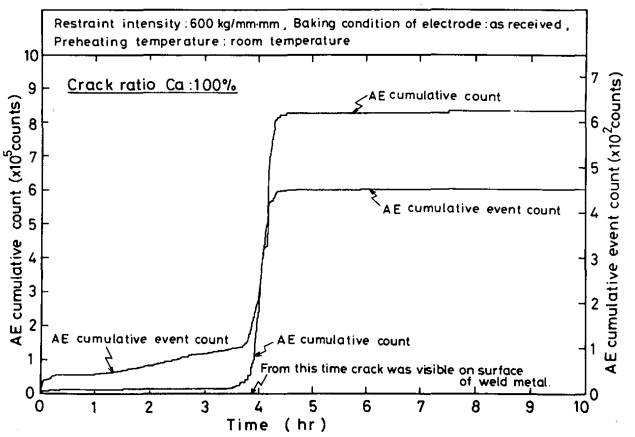

Fig. 4 Typical example of changes in AE cumulative count and cumulative event count vs. time in Group I

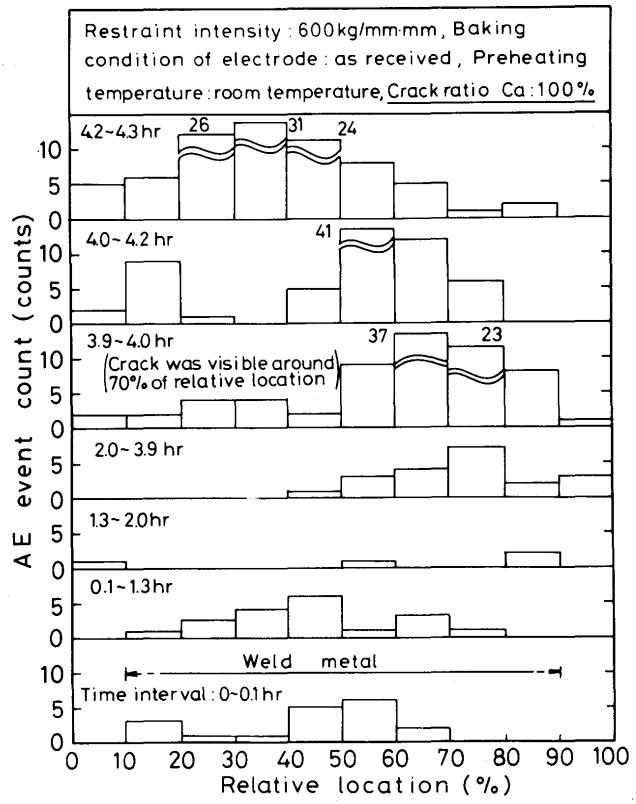

Fig. 5 Change in AE source location vs. time in the same specimen as that in Fig. 4

of measurement and thus an obvious incubation period was not observed. Both AE cumulative count and AE cumulative event count increased gradually and intermittently till about 3.9hr*. During the time intervals 0 to 3.9hr in Fig. 5 the AE events were emitted intermittently from place to place over the whole length of the weld bead. Thus it is considered that the crack had already extended over the whole length of the root at

* The increasing tendency of the AE cumulative count is obscure in Fig. 4 because of the scale of the ordinate.

3.9hr.

The AE cumulative count and the AE cumulative event count increased suddenly from about 3.9hr in Fig. 4 and the crack began to be observed with the naked eye at this moment on the surface of weld metal around 70% of the relative location, namely behind the crater. This sudden increase continued to about 4.3hr and the crack was observed in most of the length of weld bead at this time. The AE events in Fig. 5 also suddenly increased in 60 to 80% of relative location during 3.9 and 4.0hr, which agreed with the location of crack observed with the naked eye. During 4.0 and 4.3hr the AE events shifted in the decreasing direction of relative location, namely toward the starting part of weld bead and this also agreed with the propagating direction of the crack on the surface of weld metal observed with the naked eye.

The AE cumulative count and the AE cumulative event count increased slightly after about 4.3hr and the AE events scattered along the length of weld bead in the AE source location, though the change in the appearance of the surface crack was not observed. The AE after about 4.3hr is considered to be caused by linking of cracks in tiny parts which had been remaining without cracking.

The final AE source location is shown in **Fig. 6**. It

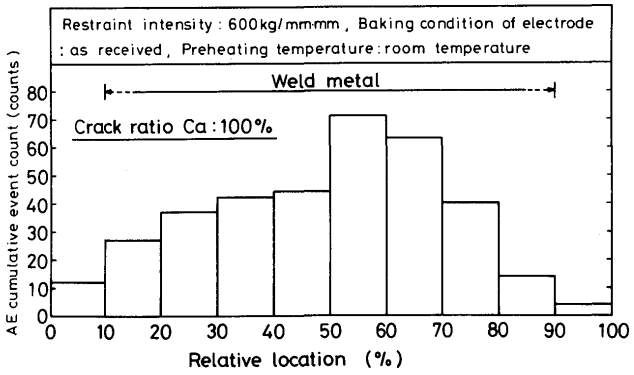

Fig. 6 Final AE source location in the same specimen as that in Figs. 4 and 5

should be noted that there are more AE events around the location where the crack reached first the surface of the weld metal. This phenomenon was observed in all the fully cracked specimen. The place where the crack reached first the surface of weld metal lay near the crater in a specimen with the low restraint intensity. That in a specimen with the medium or the high restraint intensity lay near the middle of length of the weld bead.

Besides, the time when the crack reached the surface of weld metal was shortened by increasing the restraint intensity or lowering the baking temperature of the electrode.

3.2.2 AE Source Location in Group II

As an example, **Fig. 7** shows the changes in AE

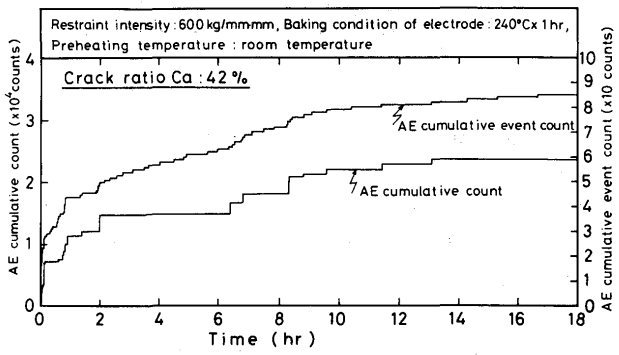

Fig. 7 Typical example of changes in AE cumulative count and cumulative event count vs. time in Group II

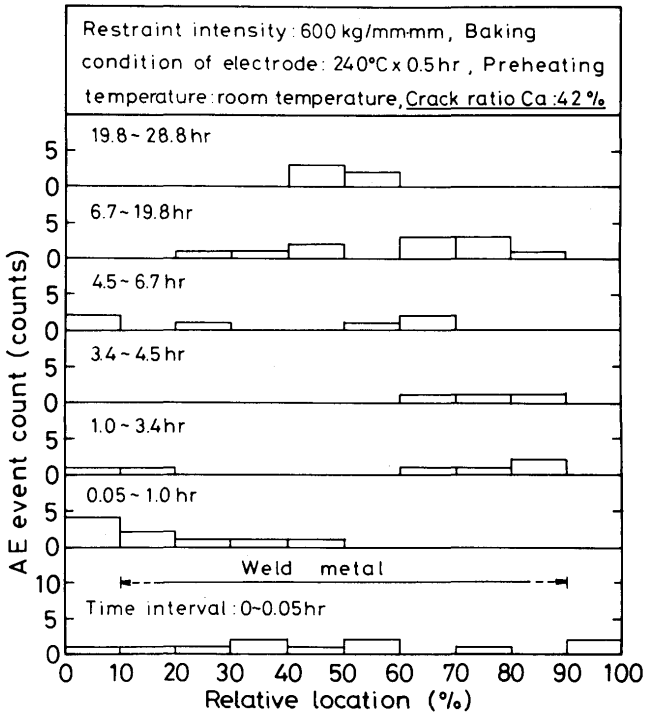

Fig. 8 Change in AE source location vs. time in the same specimen as that in Fig. 7

cumulative count and AE cumulative event count vs. time in specimen No. 6 and **Fig. 8** shows the change in AE source location in the same specimen during the time intervals shown in Fig. 8. In Fig. 7 both AE cumulative count and AE cumulative event count increased gradually and intermittently without an incubation period, and such a sudden increase as that in Fig. 4 was not observed. Moreover a large AE event was not emitted after about 14hr and any crack was not observed on the surface of weld metal even at 48hr. In Fig. 8 the AE events were emitted intermittently from place to place over the whole length of weld bead, and such a sudden increase at any

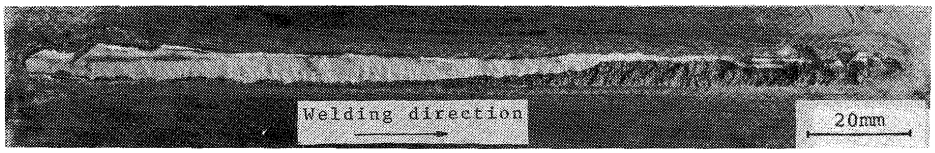

Fig. 9 Oxidized and fractured surface of the same specimen as that in Figs. 7 and 8

relative location as that in Fig. 5 was not observed. Thus it is considered that the crack extended over the whole length of the root, though the crack did not reach the surface of weld metal. **Figure 9** shows the oxidized and fractured surface, from which it is seen that the root was almost completely cracked and that the crack near the crater extended close by the surface of weld metal. The final AE source location is shown in **Fig. 10**. Neglecting

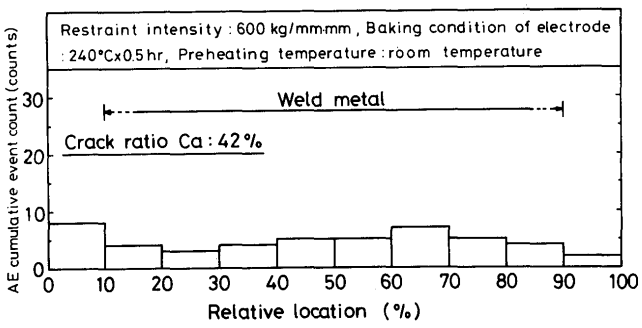

Fig. 10 Final AE source location in the same specimen as that in Figs. 7 to 9.

erroneous AE source location in 0 to 10% of relative location, there are somewhat more events in the crater side's half in the length of weld bead, which roughly accords with the distribution of crack in Fig. 9.

It should be noted that there are obvious differences in AE cumulative count and AE cumulative event count between Figs. 4 and 7, namely between Groups I and II. It should be also noted, however, that the AE cumulative count and the AE cumulative event count just before their sudden increases in Fig. 4 have similar values to those in Fig. 7. This suggests that the obvious differences in the AE data between Groups I and II are caused by the emergence of the crack on the surface of weld metal. Specimen No. 18 had fortune to prove this as follows:

Figure 11 shows the changes in AE cumulative count and AE cumulative event count vs. time in the specimen No. 18 and **Fig. 12** shows the change in AE source location during the time intervals shown in Fig. 12. In Fig. 11 both AE cumulative count and AE cumulative event count increased gradually and intermittently till about 16hr, were nearly constant from about 16 to 42hr and then increased suddenly at about 42hr, and were again constant from about 42 to 48hr. During the time intervals 0 to

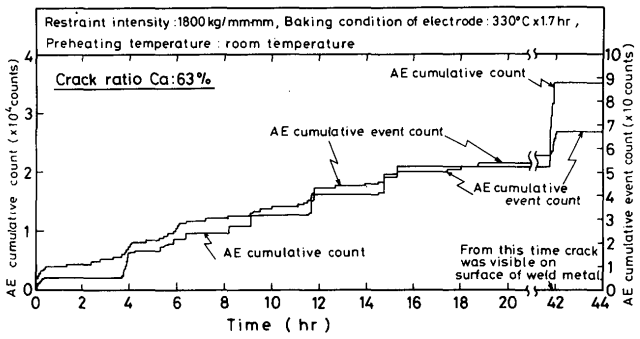

Fig. 11 Change in AE cumulative count and cumulative event count vs. time in specimen No. 18 which had a small surface crack

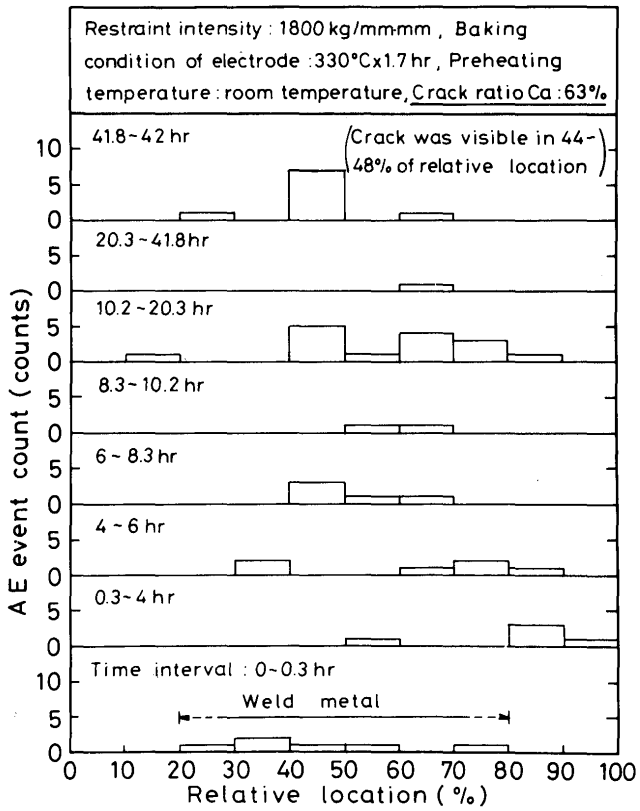

Fig. 12 Change in AE source location vs. time in the same specimen as that in Fig. 11.

41.8hr in Fig. 12 the AE events were emitted intermittently from place to place over the whole length of weld bead. Then, the AE events were concentrated in 40 to 50% of relative location at about 42hr and the crack was simultaneously observed with the naked eye in 44 to 48%

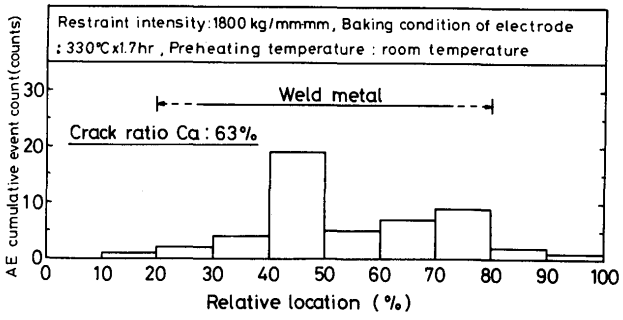

Fig. 13 Final AE source location in the same specimen as that in Figs. 11 and 12

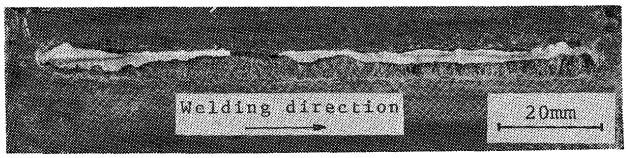

Fig. 14 Oxidized and fractured surface of the same specimen as that in Figs. 11 to 13.

of relative location of the surface of weld metal.

Figure 13 shows the final AE source location and **Fig. 14** does the oxidized and fractured surface. Comparing Fig. 13 with Fig. 14 it is recognized that many AE events were emitted at the place where the crack emerged to the surface of weld metal.

Thus, many AE cumulative counts and AE cumulative event counts, in other words many high amplitude AE bursts are emitted at crack-emerged time and at the crack-emerged place.

3.2.3 AE Source Location in Group III

As an example, **Fig. 15** shows the changes in AE cumulative count and AE cumulative event count vs. time in specimen No. 15 and **Fig. 16** shows the change in AE

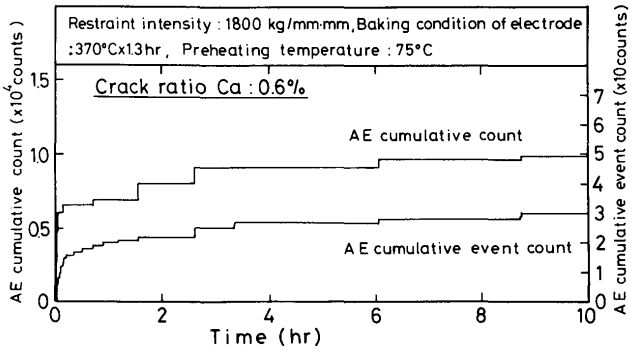

Fig. 15 Typical example of changes in AE cumulative count and cumulative event count vs. time in Group III

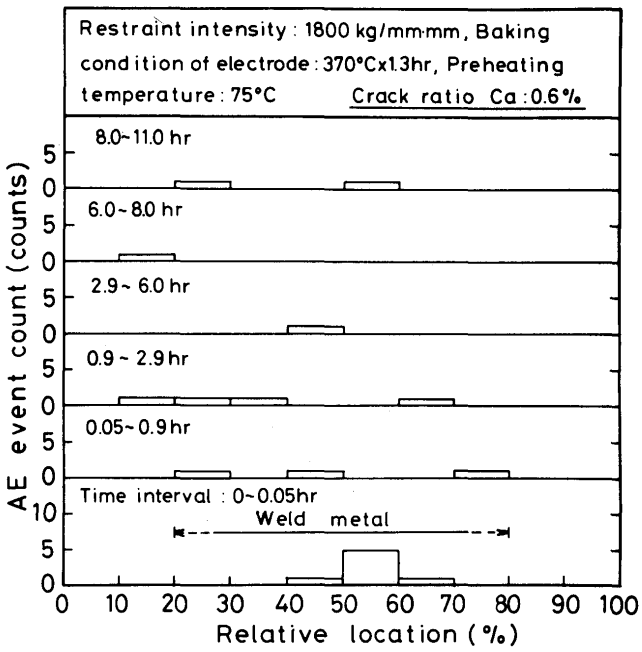

Fig. 16 Change in AE source location vs. time in the same specimen as that in Fig. 15

source location during the time intervals shown in Fig. 16. In Fig. 15 both AE cumulative count and AE cumulative event count increased gradually and a large AE event was not emitted after about 9hr. In Fig. 16 the AE events were emitted intermittently from place to place over the whole length of weld bead. **Figure 17** shows the final AE source location, and **Fig. 18** does the oxidized and

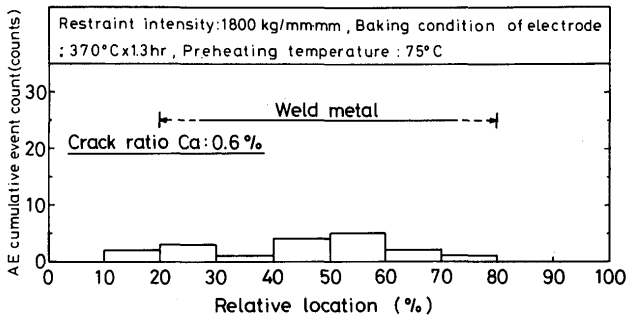

Fig. 17 Final AE source location in the same specimen as that in Figs. 15 and 16

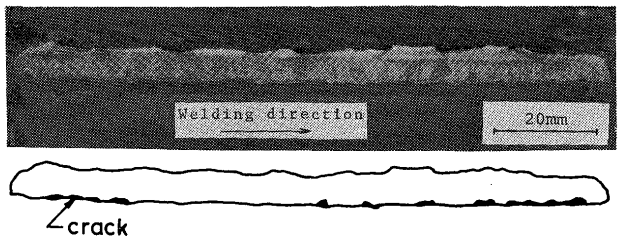

Fig. 18 Oxidized and fractured surface and its sketch of the same specimen as that in Figs. 15 to 17

fractured surface and its sketch in which the cracks are sketched exaggeratedly. It was seen in Fig. 18 that about ten cracks lay scattered along the root. The average crack size was about 0.3 to 0.5mm^2.

It should be noted that the characteristics of AE in Figs. 7, 8 and 10 in Group II resemble those in Figs. 15, 16 and 17 in Group III in spite of their obvious difference in their crack sizes. Even if other AE parameters, i.e. AE cumulative event count which is later shown in Fig. 19, AE cumulative count, S value and AE maximum ringdown counts per event which are later shown in Appendix are compared, Group III cannot be clearly distinguished from Group II by AE data, though Group I can be always easily distinguished from Groups II and III. The distinction between Groups II and III, however, can be done only from a fact that AE in Group II continued for more than 20hr and AE in Group III stops within less than 15hr neglecting small AE events having ringdown counts less than 100 counts.

3.3 Estimation of Propagation Behavior of Root Crack

Relationship between the cracked area and the final AE cumulative event count is shown in **Fig. 19**, and it is noted that the AE coumulative event counts of Group III are comparable with those of Group II.

The relationship between the cracked area and the average cracked area per event is shown in **Fig. 20**. The

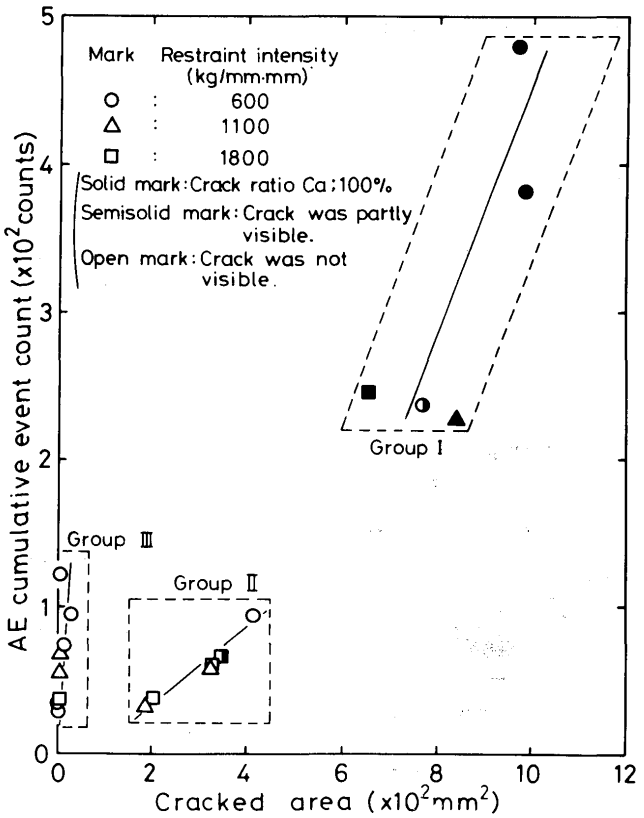

Fig. 19 Relationship between cracked area and AE cumulative event count

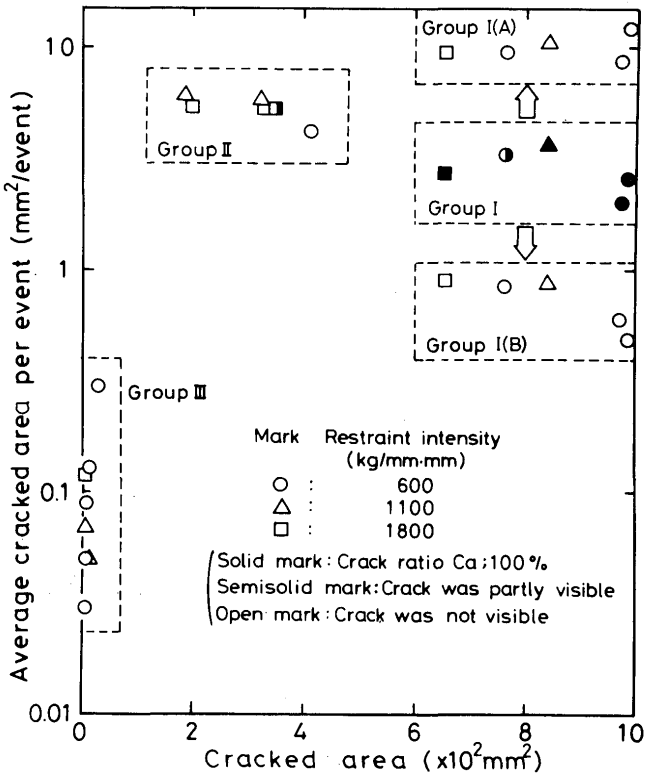

Fig. 20 Relationship between cracked area and average cracked area per event

average cracked area per event of Group I is about 3mm^2, that of Group II is about 5mm^2 and that of Group III is about 0.1mm^2. The AE characteristics of Group I, however, were composed of two stages as already mentioned. The AE in the first stage were emitted gradually and that in the second stage were emitted rapidly, which corresponded to the emergence of crack on the surface of weld metal, namely to the formation of shear lip zone. Thus, by measuring the areas of the shear lip zone and the other portion, the average cracked area per event in each stage was approximately evaluated. The average cracked area per event in the first stage is about 10mm^2 as shown in Group I(A) in Fig. 20, and that in the second stage is about 1 mm^2 as shown in Group I(B). Considering the error in this evaluation, the average cracked area per event of Group I(A) is regarded as equal to that of Group II. Kikuta et al.[7] reported that average length of crack propagation per event in slow crack growth in hydrogen-induced delayed crack was about 1 mm using a double cantilever beam specimen of 4 mm width. Therefore, it is suggested that the average cracked area per event was 4 mm^2. This well agrees with the average cracked area in Group II or I(A).

By the way, scanning electron microscope observation revealed that the crack surface of Groups I(A) and II almost consisted of hydrogen-induced quasi-cleavage fracture surface as shown in **Fig. 21 (a)**, though a small

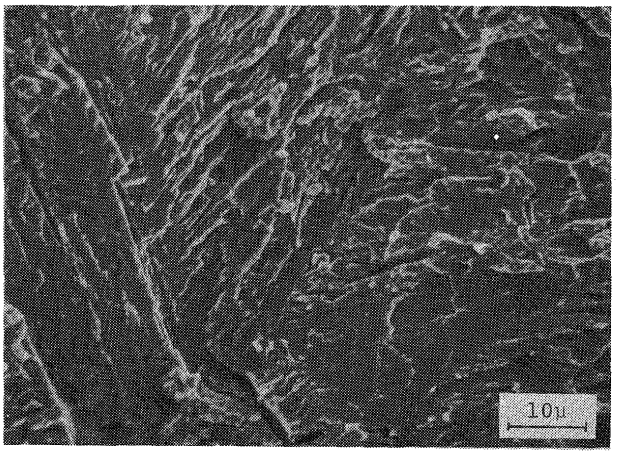

(a) hydrogen-induced quasi-cleavage fracture in heat-affected zone in Groups I and II

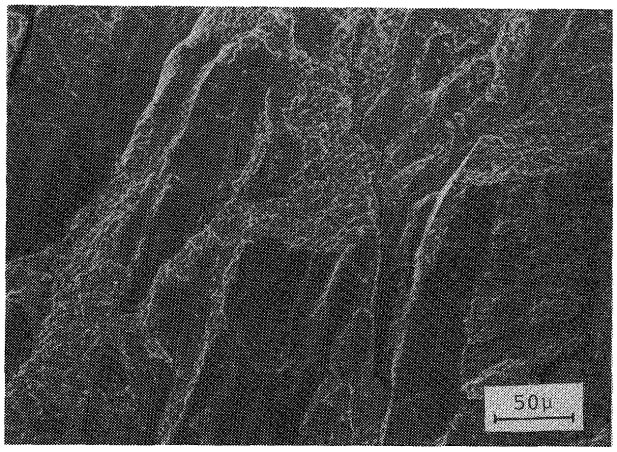

(b) mixture of intergranular and hydrogen-induced quasi-cleavage fractures in weld metal in Group I with the highest restraint intensity

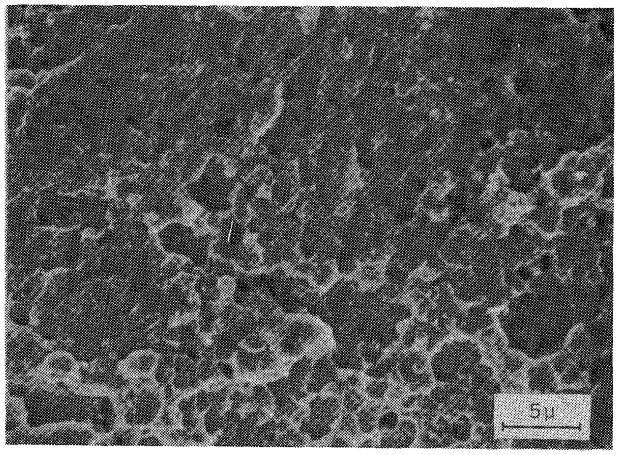

(c) shear dimple fracture in shear lip zone in weld metal in Group I

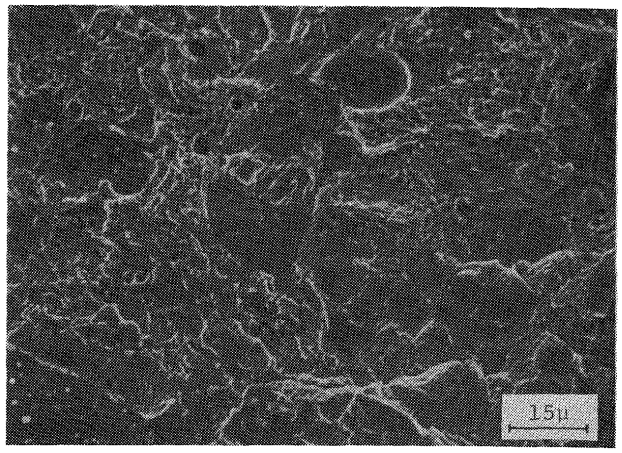

(d) mixture of intergranular, hydrogen-induced quasi-cleavage and dimple fractures in heat-affected zone in Group III

Fig. 21 Microfractographs of root crack

quantity of intergranular and dimple fracture surfaces were observed. The crack of the specimen with the highest restraint intensity propagated into the weld metal before formation of the shear lip zone as shown in Fig. 2(b), and this crack surface consisted of mixture of intergranular and hydrogen-induced quasi-cleavage fracture surfaces as shown in **Fig. 21 (b)**. The crack surface in the shear lip zone of Group I (B) consisted of shear dimple fracture surface as shown in **Fig. 21 (c)**. Thus it may be said that dimple fracture essentially causes intensive AE.

The crack surface of Group III generally consisted of mixture of intergranular, hydrogen-induced quasi-cleavage and dimple fracture surfaces as shown in **Fig. 21 (d)**. Considereing the dependence of fracture mode of hydrogen-induced crack on the hydrogen content or the applied stress[14], Fig. 21 (d) suggests that the crack of Group III grew intermittently for a long time in spite of the small crack size, which agrees with the behavior of AE in Fig. 15. This intermittent growth seems to cause many AE cumulative event counts in spite of the small crack size as shown in Fig. 19 and to cause small average cracked area per event as shown in Fig. 20. Moreover, the formation of dimple as shown in Fig. 21 (d) also may cause the many AE cumulative event counts.

Colligating all the results mentioned already, the propagation behavior of root crack is estimated as in **Fig. 22**. The root crack of Group I occurs at several sites of the root (Stage 1), propagates in order to link each other (Stages 2 and 3), and then propagates in the height direction of weld bead undergoing many steps (Stages 4 and 5). The average propagation area per step, namely per AE event is about 5mm^2 during Stages 1 to 5. Then the crack reaches a portion of the surface of weld metal as a shear lip (Stage 6), and extends over all the surface (Stage 7). The average propagating area per AE event is about

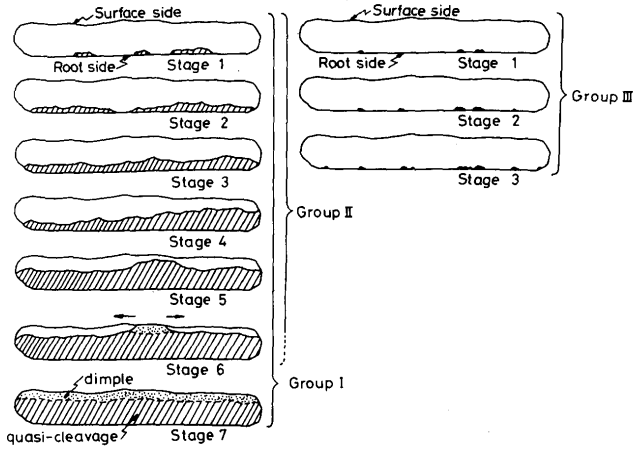

Fig. 22 Estimated propagation behavior of root crack

1 mm^2 during Stages 6 to 7.

The root crack of Group II occurs and propagates in the similar manner to that in Group I, but stops at Stage 3, 4, 5 or rarely at 6 because of the lower hydrogen content or the lower restraint intensity than in Group I.

The root crack of Group III occurs at several sites of the root in very small sizes (Stage 1). They grow a little and new cracks may occur at other sites of the root together with the lapse of time (Stages 2 to 3), and then stop. The average cracked area per AE event is about 0.1 mm^2.

4. Conclusions

AE source location technique was applied to the restraint cracking test with single bevel groove for 80kg/mm^2 class high strength steel. Main conclusions obtained are as follows:

(1) Characteristics of AE depended on crack ratios and were classified into three groups, that is Groups I, II and III. The characteristics of AE in a specimen with a large crack ratio in which there was large surface crack belonged to Group I. That in a specimen with a medium crack ratio in which there was no or a little surface crack but was nearly full crack at the root belonged to Group II. That in a specimen with a small crack ratio in which there were only some tiny cracks at the root belonged to Group III.

(2) The AE in Group I were emitted gradually and intermittently during the propagation as hydrogen-induced quasi-cleavage fracture in the heat-affected zone and then suddenly increased during the propagation as shear dimple in the shear lip zone in the weld metal. The AE in Group II were emitted gradually and intermittently for more than 20hr and then stopped, where the crack propagated as hydrogen-induced quasi-cleavage fracture in the heat-affected zone. The AE in Group III were similar to those in Group II but stopped within less than 15hr, where the crack propagated as a mixture mode of intergranualr, hydrogen-induced quasi-cleavage and dimple fractures in spite of the small crack size.

(3) Average cracked area per AE event was about 5 mm^2 during the crack propagation as hydrogen-induced quasi-cleavage fracture in the heat-affected zone in Groups I and II. That was about 1 mm^2 during the crack propagation as shear dimple fracture in Group I. That was about 0.1 mm^2 in Group III.

(4) Propagation behavior of the root crack was estimated with the aid of AE source location technique etc. The root crack of Group I occurs at several sites of the root, propagates in order to link each other and then in the height direction of weld bead, reaches a portion of the surface of weld bead, and further extends over all the surface. The root crack of Group II occurs and propagates in the similar manner to that in Group I, but stops before reaching the surface. The root crack of Group III occurs at several sites of the root, and they grow a little and new cracks may occur at other sites of the root and then stop before linking each other completely.

(5) Any of AE cumulative count, cumulative event count, S value which is the slope of ringdown counts distribution and maximum ringdown counts per event could easily distinguish Group I from Groups II and III, because many intensive AE were emitted in Group I when the crack reached the surface of weld metal. However, any of these AE parameters could not distinguish between Groups II and III, excepting the difference in sustaining time of AE mentioned in conclusion (2).

Acknowledgement

The authours would like to thank Osaka Transformer Corp. Ltd. for the performance of restraint welding with electron beam welding.

References

1) C.E. Hartbower, et al.: ASTM STP-505 (1971), pp. 187-221.
2) E. Isono, et al.: J. NDI, Vol. 21 (1972), pp. 226-233 (in Japanese).
3) B.S. Kasatkin, et al.: Avt. Svarka, Vol. 25 (1972), pp. 32-35.
4) J. Tsuboi, et al.: J. Japan Weld. Soc., Vol. 45 (1976), pp. 574-581 (in Japanese).
5) Y. Hirai, et al.: J. Japan Weld. Soc., Vol. 45 (1976), pp. 634-640 (in Japanese).
6) N. Ogura, et la.; J. Japan Weld. Soc., Vol, 47 (1978), pp. 638-643 (in Japanese).
7) Y. Kikuta, et al.: J. Iron & Steel Inst. Japan, Vol. 64 (1978), pp. 538-567 (in Japanese).
8) C.E. Hartbower, et al.: Weld. J., Vol. 47 (1968), 1s-18s.
9) H.L. Dunegan, et al.: Eng'g Fracture Mechanics, Vol. 2 (1971), pp. 387-402.

10) F. Matsuda, et al.: Trans. JWRI, Vol. 7 (1978), No. 1, pp. 87-92.
11) W.P. Campbell: Weld. J., Vol. 55 (1976), 135s-143s.
12) Y. Ueda, et al.: Trans. JWRI, Vol. 7 (1978), No. 1, pp. 11-16.
13) H. Nakasa, et al.: 3rd AE Symp., 1976 (Tokyo), pp. 131-151.
14) C.D. Beachem: Met. Trans., Vol. 3 (1972), pp. 437-451.

Appendix

Relationship between Cracked Area and AE Parameters

A-1. AE Cumulative Count vs. Cracked Area

The relationship between the cracked area and the AE cumulative count is shown in **Fig. A-1**. It should be noted that the AE cumulative counts in Group III are comparable with those in Group II, but the reason is incomprehensive for the present. The relationship in Fig. A-1 resembles to that in Fig. 19 which shows the relationship between the cracked area and the AE cumulative event count. Therefore the distinction between Groups II and III is impossible, though Group I can be easily distinguished from Groups II and III.

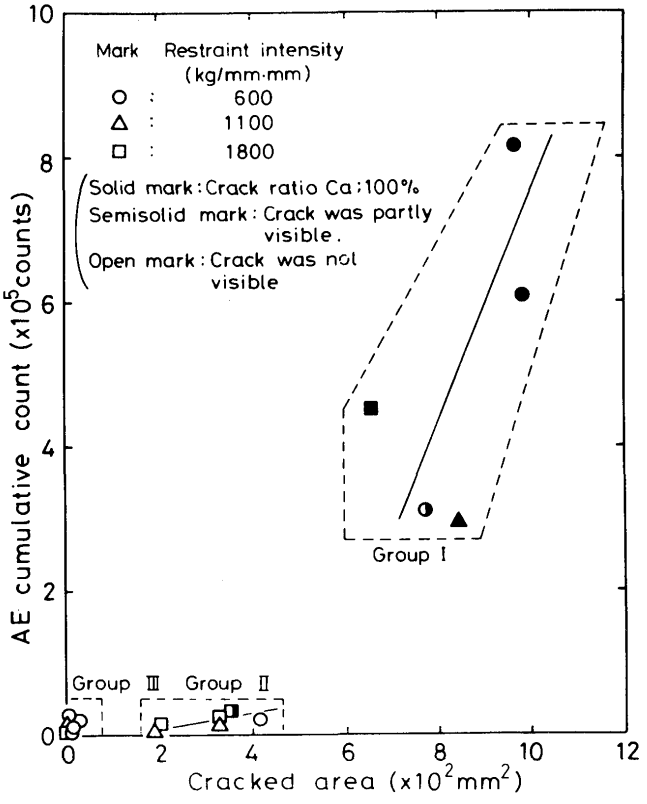

(a) general figure

Fig. A-1 Relationship between cracked area and AE cumulative count

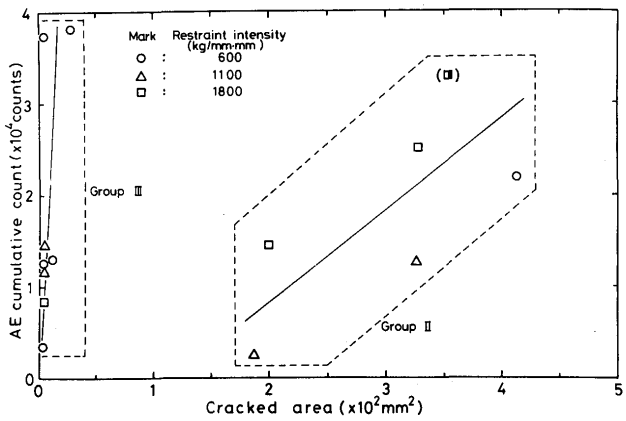

(b) magnified figure in lower left in (a)

A-2. SValue vs. Cracked Area

Examples of ringdown counts distribution are shown in **Fig. A-2**, where the ordinate is the sum of AE events which have ringdown counts exceeding a given value in the abscissa. The S value is defined to be the average slope of the ringdown counts distribution. Small S value means that there are many AE events having large ringdown counts. In Fig. A-2 S value in crack ratio Ca 100% is smaller than that in crack ratio Ca 51%. An example of change in S value during the crack propagation in a specimen of crack ratio Ca 100% is shown in **Fig. A-3**. S value has a decreasing tendency as a whole during the crack propagation, though having sudden drops and slight increase between them. It is interesting that an especially sudden drop of S value occurred just before the time from which crack was visible on the surface of weld metal.

The relationship between the cracked area and S value is shown in **Fig. A-4**, where Group I can be distinguished

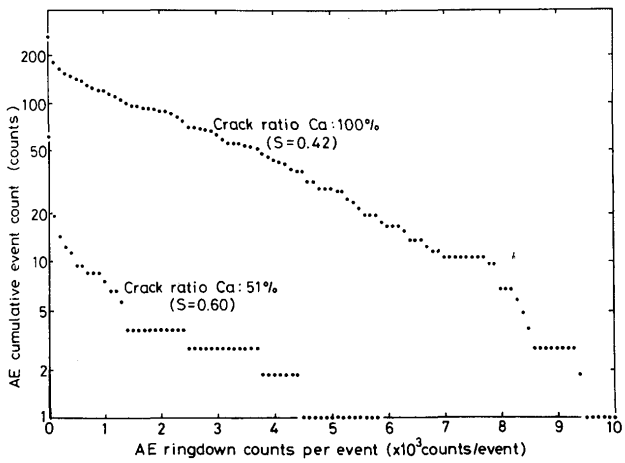

Fig. A-2 Examples of AE ringdown counts distribution

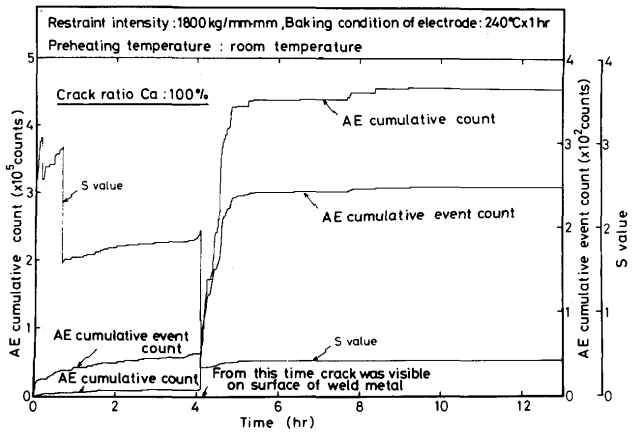

Fig. A-3 Change in S value together with AE cumulative count and cumulative event count vs. time

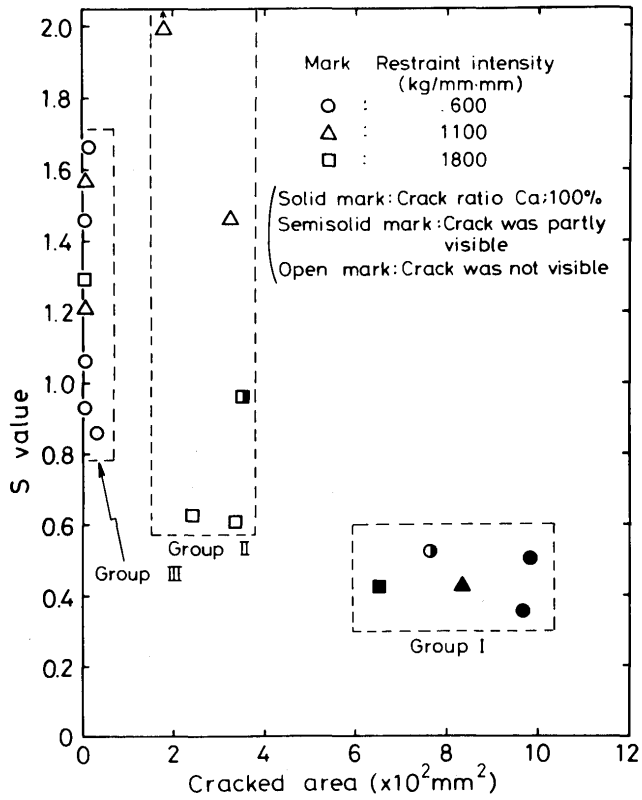

Fig. A-4 Relationship between cracked area and S value

from Groups II and III by S value, but the distinction between Groups II and III is impossible.

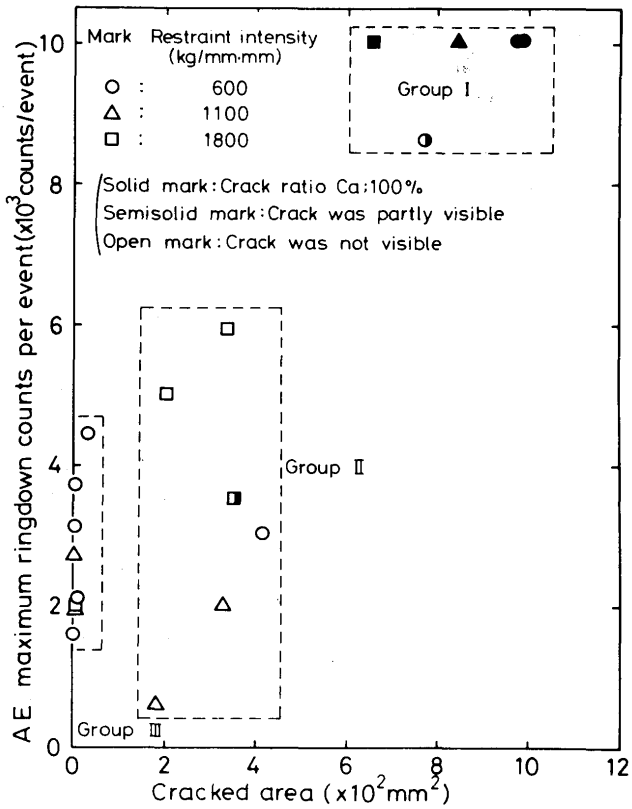

Fig. A-5 Relationship between cracked area and AE maximum ringdown counts per event.

A-3. Maximum Ringdown Counts per Event

It is considered roughly that the value of ringdown counts of a AE burst is related to the amplitude. The maximum value can be read on the abscissa of ringdown counts distribution shown in Fig. A-2. The relationship between the cracked area and the maximum ringdown counts per event is shown in **Fig. A-5**, where the distinction between Groups II and III is also impossible.

A-4. Estimation of Cracked Area from AE Parameters

As already mentioned in 3.2.3, the distinction between Groups II and III is barely possible using the difference in sustaining time of AE. Therefore, distinguishing among Groups I, II and III by the sustaining time of AE and other AE parameters, the cracked area can be roughly estimated by AE cumulative event count in Fig. 19 or by AE cumulative count in Fig. A-1.